

Realization of Stair Ascent and Motion Transitions on Prostheses utilizing Optimization-Based Control and Intent Recognition

Huihua Zhao
Mechanical Engineering
Georgia Institute of Technology
Atlanta, GA 30332
Email: huihua@gatech.edu

Jacob Reher, Jonathan Horn, Victor Paredes
Mechanical Engineering
Texas A&M University
College Station, TX 77843
Email: {jreher,j.horn,vcparedesc}@tamu.edu

Aaron D. Ames
Mechanical Engineering
Electrical & Computer Engineering
Georgia Institute of Technology
Email: ames@gatech.edu

Abstract—This paper presents a systematic methodology for achieving stable locomotion behaviors on transfemoral prostheses, together with a framework for transitioning between these behaviors—both of which are realized experimentally on the self-contained custom-built prosthesis AMPRO. Extending previous results for translating robotic walking to prosthesis, the first main contribution of this paper is the gait generation and control development for realizing dynamic stair climbing. This framework leads to the second main contribution of the paper: a methodology for motion intent recognition, allowing for natural and smooth transitions between different motion primitives, e.g., standing, level walking, and stair climbing. The contributions presented in this paper, including stair ascent and transitioning between motion primitives, are verified in simulation and realized experimentally on AMPRO. Improved tracking and energy efficiency is seen when the online optimization based controller is utilized for stair climbing and the motion intent recognition algorithm successfully transitions between motion primitives with a success rate of over 98%.

I. INTRODUCTION

According to the National Center for Health Statistics approximately 222,000 people in the United States are transfemoral amputees [1]. Their daily life is greatly limited by the use of energetically passive prostheses. While the development of passive devices has achieved stable level ground walking, reports indicate that the amputees using them have increased metabolic costs and exert as much as three times the affected-side hip power and torque [2]. More importantly, stair climbing—one common activity of daily living for able-bodied persons—remains a challenging task for transfemoral amputees. As a means to address the shortcomings of passive devices, powered prostheses capable of providing net power in conjunction with various prosthesis controllers have been developed in recent decades to achieve successful human-like powered flat-ground walking [3], [4], [5]. However, to the knowledge of the authors, the implementation of stair ascent with a powered knee and ankle transfemoral prosthesis is limited and only found in [6], [7] with the use of variable impedance control. This motivates the first main contribution of this paper.

The authors' previous work has reported a systematic methodology for using bipedal robots to test prosthetic controllers with the goal of potentially reducing the cost of clinical testing for prostheses and expediting the development of optimal controllers [8], [9]. In particular, a nominal walking gait was found for the robot platform which displays

qualitatively human-like walking, and prosthetic controllers were tested on a “leg” of the robot [9]. Through this method, a novel on-line optimization-based transfemoral prosthesis control method: control Lyapunov function (CLF) based quadratic programs (QPs), coupled with variable impedance control, is tested and verified on the bipedal robot AMBER. This synergistic method was then translated to a custom-built self-contained transfemoral prosthetic device to achieve level walking [8]. In this paper, the first contribution is the extension of the described framework from walking on flat ground to stair ascent, yielding both prosthesis gait generation and on-line optimal controller to realize these gaits on the device. Through experimental testing, the on-line optimal control framework is compared to traditional control methodologies. The results indicate both improved tracking and energy efficiency.

Another fundamental advantage of powered prostheses is that these devices are capable of interacting with the user in intelligent and natural ways, while passive devices can only assist the user with a predefined routine. In order to realize the potential of powered prostheses, an intention interface is necessary to allow the user to control the device through different motion behaviors, i.e., switching between different motion primitives. Proposed approaches include using mechanical triggers or compensatory body movements [10]. However, more natural and smooth motion switching strategies are found when utilizing pattern recognition algorithms which, for example, have been realized successfully in [7], [11], [12]. Motivated by the goal of making the proposed framework practically applicable to prosthesis users, the second main contribution of this paper is a simple yet effective motion intent recognition algorithm using a neural network classifier. Exploiting the advantages of an instrumented healthy leg and a switch-score scheme, the method is able to accomplish motion switches between 3 motion primitives (including standing, level walking and stair ascent) naturally with minimum delay. More importantly, for one switch mode, the total time cost from static database training to real-time implementation is less than 30 minutes including minimum tuning on the switch-score scheme. The motion intent algorithm is able to predict the motion transition with 1 failure during the total of 56 switch tests, i.e., the accuracy is above 98%.

The structure of this paper is as follows: the automatic prosthetic gait generation method is introduced in Sec. II.

A three-level hierarchical control architecture, including the intention recognition, is discussed in Sec. III. The experimental realization of the nonlinear real-time optimization based controller on a prosthesis for stair ascent is illustrated in Sec. IV. Motion transitions with the proposed intention recognition is also tested in this section. Conclusions and future work are presented at the end.

II. PROSTHETIC GAITS GENERATION

With the goal of designing a prosthetic gait utilizing robotic models, a hybrid system model with anthropomorphic parameters is considered in this section. An optimization problem is then introduced for automatic gait design.

A. Motion Capture with IMU

In an effort to achieve natural human-like prosthetic walking for a transfemoral amputee, a low-cost inertial motion capture system with IMUs is developed to collect healthy human locomotion data. A model based Extended Kalman Filter (EKF) [13] is introduced to obtain accurate joint angle information about the human subject. During the experiments, the subject was asked to walk along a straight line or ascend a staircase (with 10 cm stair height) in a flat-footed gait for several steps, the data of which are averaged to yield the unique trajectories for optimization [8]. The human trajectories captured by the IMUs are compared with camera motion capture data (with 25 cm stair height) obtained from UC Berkley Motion Capture Lab [14]. The results shown in Fig. 1 indicate that the IMU system is able to capture the human locomotion trajectory quantitatively with the differences between the trajectories largely due to the stair height difference in the two experiments (10 cm vs. 25 cm); this affects peak swing knee angle. Finally, note that these differences will not significantly affect the gaits generated since the human data only seeds the optimization problem that yields gaits for the prosthesis.

B. Gait Generation For Prostheses

With the reference human trajectories collected, the next step is to design a prosthetic gait that is specific to the individual user and the particular prosthetic device. A planar bipedal robot with anthropomorphic parameters is considered to be the “human” model for the purpose of gait design. Based on this model and the human locomotion data obtained with the IMUs, the human-inspired optimization [15] is implemented to generate a human-like gait that is both stable and optimal for the prosthetic device.

Robot Model. Due to the presence of discrete behavior in walking, i.e., due to impacts that result from foot strike, we represent a bipedal robot as a hybrid system with configuration space Q_R with the coordinates given as: $\theta = (\theta_{sa}, \theta_{sk}, \theta_{sh}, \theta_{nsh}, \theta_{nsk}, \theta_{nsa})^T$ as shown in Fig. 2. The equations of motion of the continuous dynamics are obtained using the Euler-Lagrange formula:

$$D(\theta)\ddot{\theta} + H(\theta, \dot{\theta}) = Bu, \quad (1)$$

where $D(\theta) \in \mathbb{R}^{6 \times 6}$ is the inertial matrix and $H(\theta, \dot{\theta}) \in \mathbb{R}^{6 \times 1}$ contains the terms of the Coriolis effect and the gravity

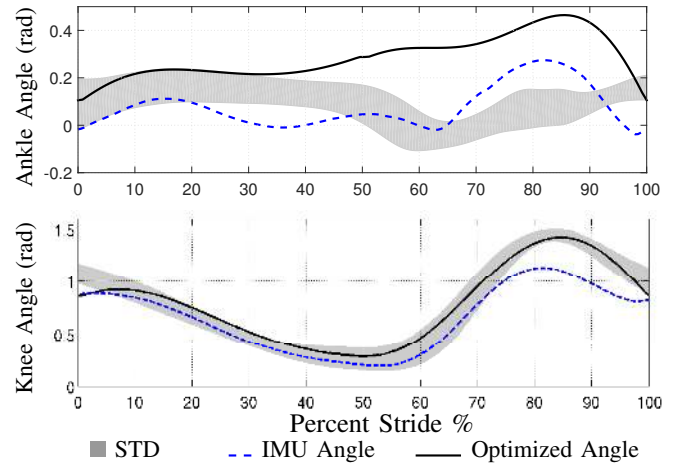


Fig. 1: Average angles for human subject and the optimized angles as compared to the one standard deviation (STD) of camera motion captured data [14].

vector. The torque map $B = I_6$ and the control input, u , is the vector of torque inputs; more details can be found in [15].

Aiming to achieve human-like robotic walking, we consider the “complex” human locomotion system as a “black box.” Therefore, the goal becomes to drive the actual robot outputs $y^a(\theta, \dot{\theta})$ to the desired human outputs $y^d(t, \alpha)$ that are represented by a specific walking function characterized by a parameter set α [15]. The objective then becomes to drive the error $y(\theta, \dot{\theta}, \alpha) = y^a(\theta, \dot{\theta}) - y^d(t, \alpha) \rightarrow \mathbf{0}$. With these outputs (i.e. virtual constraints), the human-inspired controller as discussed in [15] can be utilized to drive $y \rightarrow 0$ in a provably exponentially stable fashion for the continuous dynamics. However, the robot will be “thrown-off” the designed trajectory when impacts occur. This motivates the introduction of the *partial hybrid zero dynamics* (PHZD) constraints aiming to yield a parameter set α that ensures the tracking of position based outputs will remain invariant and smooth even through impacts. In particular, with the *partial zero dynamics* (PZD) surface defined as:

$$\mathbf{PZ}_\alpha = \{(\theta, \dot{\theta}) \in Q_R : y_2(\theta, \alpha) = \mathbf{0}, \dot{y}_2(\theta, \alpha) = \mathbf{0}\}, \quad (2)$$

where $y_2(\theta, \alpha)$ is the position based outputs as discussed in [15], the PHZD constraints can be stated as:

$$\Delta_R(S_R \cap \mathbf{PZ}_\alpha) = \mathbf{PZ}_\alpha, \quad (\text{PHZD})$$

where Δ_R and S_R are the reset map and switching surface of the robot model, respectively. A detailed explanation of these constraints can be found in [15], [16].

Human-Inspired Optimization. By enforcing the PHZD constraints discussed above, a human-inspired optimization is utilized to generate walking trajectories that are both provably stable and kinematically human-like [15], [17]. More importantly, a lower-limb prosthesis must interact with humans in a safety-critical fashion, thus more attention should be placed on physical constraints that relate to safety (e.g., hardware limits) and energy conservation (power consumption). These specifications yield the optimization

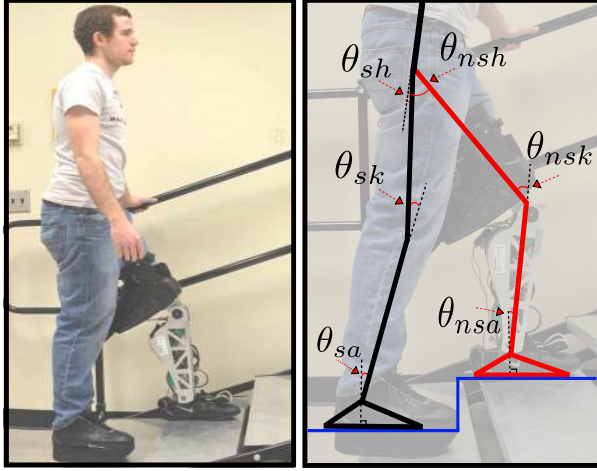


Fig. 2: Human subject with AMPRO and the robotic model.

problem subject to both PHZD and physical constraints:

$$\begin{aligned} \alpha^* = \operatorname{argmin}_{\alpha \in \mathbb{R}^{26}} \operatorname{Cost}_{\text{HD}}(\alpha) \quad (3) \\ \text{s.t. (PHZD) Constraints,} \\ \text{Physical Constraints,} \end{aligned}$$

where the cost function is the least-square-fit error between the human experimental data and the chosen walking function [14]. The end result of this optimization problem is the parameter set α that renders an optimal¹ (w.r.t. torque, foot clearance, joint position and velocity) and provably stable human-like stair ascent gait, which can be implemented directly on the prosthetic device. The stability of the stair climbing gait obtained through the optimization was numerically validated through the Poincaré map [18], wherein the magnitude of the maximum eigenvalue was found to be 0.069, indicating the stability.

To summarize, utilizing the trajectory of a healthy subject as the reference, this optimization problem is subject to both the PHZD constraints to ensure smooth transitions and the physical constraints for torque and angle limitations, such that the output gait is applicable for implementation on the prosthetic device. Therefore, the main advantages of utilizing this optimization problem are twofold: a) an optimal smooth subject-like gait can be designed for a specific amputee without hand tuning and, b) the output gait can be practically implemented on the prosthetic device directly while theoretically guaranteeing optimality.

III. CONTROLLER CONSTRUCTION

The architecture of the control scheme for the powered transfemoral prosthesis includes three hierarchical levels, as in Fig. 3. The low-level controller is realized in a closed-loop by the ELMO motion drive, which is able to compensate for the friction, damping effects and transmission dynamics. The mid-level controllers generate the input torques for the joints

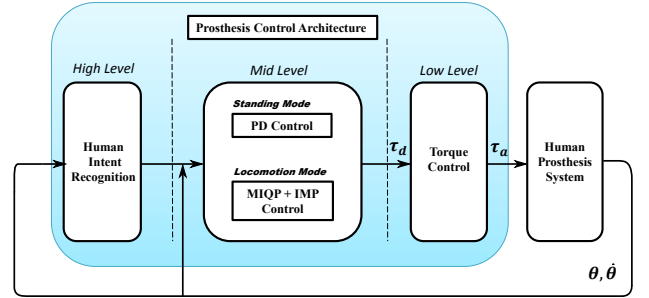


Fig. 3: Hierarchical control architecture of AMPRO.

using various controllers. In particular, the motion primitives of flat-ground walking and stair climbing will be controlled using a real-time quadratic program based controller as described in [8], and a PD controller is utilized for the standing mode control. The high-level controller predicts the intent of the motion, and switches to the appropriate mid-level controller accordingly.

A. MIQP+Impedance Control

In previous work [8], the authors proposed a novel prosthetic controller that combines the *rapidly exponentially stabilizing control Lyapunov functions* (RES-CLFs) based quadratic program control [19] with impedance control in an effort to achieve better tracking and improved energy efficiency on prostheses. In particular, using the human-inspired feedback linearization controller [15], the equation (1) can be converted to a linear form as follows:

$$\dot{\eta} = \underbrace{\begin{bmatrix} 0_{2 \times 2} & I_{2 \times 2} \\ 0_{2 \times 2} & 0_{2 \times 2} \end{bmatrix}}_F \eta + \underbrace{\begin{bmatrix} 0_{2 \times 2} \\ I_{2 \times 2} \end{bmatrix}}_G \mu, \quad (4)$$

where $\eta = (y_p; \dot{y}_p) \in \mathbb{R}^{4 \times 1}$ with $y_p = (\theta_a^p, \theta_k^p)^T$ the angles for the prosthetic ankle joint and knee joint, respectively. Leveraging the Continuous Algebraic Riccati Equation (CARE) with solution $P = P^T > 0$, allows for the construction of a RES-CLF [19] given as:

$$V_\varepsilon(\eta) = \eta^T \begin{bmatrix} \frac{1}{\varepsilon} I & 0 \\ 0 & I \end{bmatrix} P \begin{bmatrix} \frac{1}{\varepsilon} I & 0 \\ 0 & I \end{bmatrix} \eta := \eta^T P_\varepsilon \eta, \quad (5)$$

with convergence rate $\varepsilon > 0$ [19]. In order to exponentially stabilize the system, we want to find μ such that, for a chosen $\gamma > 0$ [19], we have:

$$L_F V_\varepsilon(\eta) + L_G V_\varepsilon(\eta) \mu \leq -\frac{\gamma}{\varepsilon} V_\varepsilon(\eta), \quad (6)$$

where $L_F V_\varepsilon(\eta)$ and $L_G V_\varepsilon(\eta)$ are the corresponding Lie derivatives of the Lyapunov function (5) relative to the dynamics in (4). Since this constraint is affine in μ , it can naturally be utilized in a quadratic program (QP) to achieve (point-wise) optimal choices of μ . More importantly, we add the impedance term μ^{imp} into this construction for the total hardware torque bounds, which yields the following

¹Here “optimal” refers to local optimality assuming convergence of (3); since the constraints are nonlinear, global optimality cannot be guaranteed.

model independent quadratic program plus impedance control (MIQP+Impedance):

$$\begin{aligned}
& \underset{(\delta, \mu^{qp}(\eta)) \in \mathbb{R}^{2+1}}{\operatorname{argmin}} && p\delta^2 + \mu^{qpT} \mu^{qp} && (7) \\
& \text{s.t.} && L_F V_\varepsilon(\eta) + \frac{\gamma}{\varepsilon} V_\varepsilon(\eta) + L_G V_\varepsilon(\eta) \mu^{qp} \leq \delta, \text{ (CLF)} \\
& && \mu^{qp} \leq \mu_{MAX}^{qp}, && \text{(Max QP Torque)} \\
& && -\mu^{qp} \leq \mu_{MAX}^{qp}, && \text{(Min QP Torque)} \\
& && \mu^{qp} \leq \mu_{MAX} - \mu^{imp}, && \text{(Max Input Torque)} \\
& && -\mu^{qp} \leq \mu_{MAX} + \mu^{imp}, && \text{(Min Input Torque)}
\end{aligned}$$

where δ is a relaxation factor that ensures that hardware constraints (related to torque) take priority over control objectives. This QP problem yields an optimal controller that regulates the error in the output dynamics in a model-independent rapidly exponentially convergence fashion. Simultaneously, by adding the impedance control as a feed-forward term into the input torque, the model independent dynamic system (4) gathers some information about the system that it is controlling. We can also set the total input torque bounds such that the optimization-based control law will generate torques that respect the hardware torque bounds μ_{MAX} , which is critical for practical implementation.

This nonlinear optimal control was first verified in simulation [20] and then on a bipedal robot: AMBER, which has been shown to achieve stable “prosthetic” walking [9]. After being verified on the “human-like” robot platform, the systematic methodology including the gait generation method and the proposed controller was then translated to a custom-built prosthetic device—AMPRO—for flat-ground walking [8]. Stable and robust prosthetic flat-ground walking in both the laboratory and real-world environments has been achieved. More importantly, the proposed real-time optimal controller also outperforms other existing controllers (such as PD) w.r.t. both tracking (23% improvement) and power consumption (25% reduction). This work will extend the aforementioned previous results in two novel ways: (1) the real-time optimization-based controller will be utilized to achieve stair climbing both in simulation and experimentally on the prosthesis AMPRO, and (2) motion transitions between three motion primitives—standing, walking and stair climbing—will be realized with the optimization-based controller serving as the mid-level controller.

B. High-Level Intent Recognition

The high-level recognition is realized using a pattern recognizer that combines neural network models for classification and a switch-score scheme for switching, which will be discussed in this section.

Neural Network Classification. Neural network has been a popular data-driven self-adaptive classification algorithm for nonlinear models [21]. Mature commercial algorithms are available for fast development, which is one of the reasons why the neural network model is chosen as the classification method for this work. In particular, for the three motion primitives considered in this paper—standing (SD), level walking (LW) and stair ascent (SA), the following motion

transitions are considered for these primitives: the switch from LW to SD, from SA to SD and from SD to LW or SA. All the models will be trained with separate databases, which will be discussed in detail in Sec. IV.

Switch-Score Scheme. The confidence of the switching algorithm can be greatly improved by adopting a switch-score scheme. In particular, the switch-score scheme includes two steps. For the first step, the forward hip position is used as a threshold to trigger the motion intent recognition algorithm. For example, the transition from SD to LW or SA will be started only if the hip position is greater than zero. Once the motion switch model is triggered, a switch-score for the model will add up if a particular motion is detected continuously. The motion primitive will switch when the switch-score reaches a threshold. Note that this strategy saves computation time (the intent recognition algorithm runs only when a specific condition is satisfied) and increases the classification accuracy (because the target motion is checked constantly for a customized timing window to reduce the possibility of miss-classification as much as possible).

IV. EXPERIMENTAL IMPLEMENTATION

With the gait generated in Sec. II and the control architecture introduced in Sec. III, we now have the framework to realize the main contributions of this paper experimentally on the custom-built prosthesis AMPRO: (1) the real-time optimization based controller for the dynamic motion primitives walking and stair ascent and (2) realization of motion transitions between the three primitives considering in this paper: standing, walking and stair climbing.

A. Experiment Setup with AMPRO

AMPRO (AMBER Prosthetic) is a custom designed self-contained transfemoral prosthetic device, which includes two brushless DC motors to actuate both the ankle and knee joints in the sagittal plane. More details about the design specifications can be found in [8]. To provide a point of human-robotic interaction, two IMUs are mounted on the shin and thigh of the human leg. The EKF model (see Sec. II) for each IMU is used to obtain the angle/velocity of both the ankle and knee, which is directly used for control purposes (see details in [8]).

B. Motion Recognition with Neural Network

To train the neural network models properly, a database of the mechanical sensor data from both the healthy leg and the prosthetic leg, via IMUs and encoders, respectively, are collected. During the database collection experiment, the test subject was asked to perform ten trials for each task, which includes transitions from SD to LW, from LW to SD, from SD to SA and from SA to SD. The labeling process is supervised by a knee angle threshold of the healthy human leg. In particular, when the swing knee angle is smaller than the threshold, the data is considered to be the source motion primitive of the transition. Otherwise, the data is labeled as the target motion primitive of the transition. With the labeled database, the neural network models are trained with the guidance of Occam’s Razor principle [21]. With

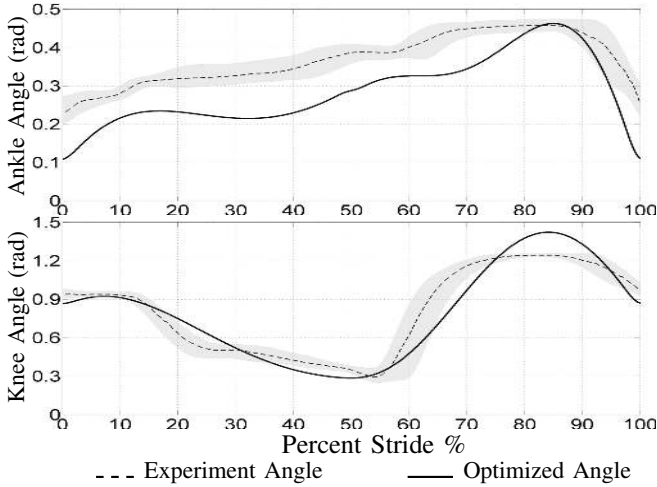


Fig. 4: Averaged experimental joint angles compared with the designed joint angles obtained from optimization. Grey area is the one standard deviation of the experiment results.

the guarantee that performance is similar between different candidate models, the simplest model is chosen in order to avoid over-fitting. In particular, all the finalized three models are chosen to have only one hidden layer. For the two-class classification models, 4 hidden neurons are used. For the three-class classification model, a total number of 10 hidden neurons are considered. The trained models are then used for real-time motion recognition in the high-level control.

C. Experimental Results

A PD controller is first realized to track the reconstructed trajectories obtained in Sec. II to achieve stair ascent. The walking trials were performed on a stair case with 10 cm stair height. The impedance parameters are then estimated using the least-square fitting method based on the experimental stair climbing data obtained using the PD controller.

Stair Ascent Implementation. With the impedance parameters, we apply the impedance control as the feed-forward term while using the MIQP as the feedback to track the desired joint trajectories. The resulting joint trajectories are averaged and compared with the designed joint angles as shown in Fig. 4, from which we can see that the actual prosthetic walking can replicate the designed trajectory very well. A video of the resulting behaviors can be seen at [22].

In order to show the optimality of the proposed optimal

controller, a PD+Impedance control that combines the PD control and impedance control is tested and compared. Note that, with the MIQP controller, physical torque bounds can be considered directly in the quadratic program [8]. Therefore, the optimal torque will satisfy the torque bounds automatically. For the first round of testing, the torque bounds are set to be 80 Nm (MIQPH+Imp) due to the safety concerns. With the goal of showing improved efficiency of the proposed novel controller (7), the torque bounds are reduced to 50 Nm (MIQPL+Imp) in the second round of testing. The experiment results are listed in the Table I (calculated from 3 rounds of experiments).

Intent Recognition Verification. With the optimal controller verified for both LW and SA, the pattern recognition algorithm is successfully realized on the prosthesis. To test the effectiveness of the motion intent recognition algorithm, a total of 14 tests are carried. In each round of the test, the subject was asked to start from SD, take 3 steps of LW, switch to SD, then continue to SA for 3 steps, finally stopping at SD posture. During the total of 56 switches, only one failed when the subject tried to start from SD to LW. Experimental gait tiles including stair ascent and motion transitions are shown in Fig. 5. The experiment results of the motion transitions are shown in the attached video [22].

D. Discussion

Due to the flat-foot assumption, the prosthetic ankle does not provide significant power during the gait. Therefore, the discussion will be mainly focused on the knee joint, which provides most of the torque and power that are required for stair ascent. From the tracking results shown in Table I, we can conclude that tracking performances of the knee are the best for MIQPH+Imp control. In addition to an improved tracking performance (61.8% improvement for the rms error e_{rms} and 46.3% for the max error e_{max}), the power consumption of MIQPL+Imp control is also less (14.5% reduction) when compared to the PD+Impedance controller.

From the perspective of power consumption, the PD controller actually has the lowest power consumption. We argue that it is because of that the PD controller fails to provide qualitative performance (sufficient power) during the SA. In particular, for SA, there is a net knee extension in stance (from 1.0 rad at the beginning to 0.2 rad at the end of stance phase) to lift the user up to the stairs. However, the PD controller failed to lift the user up effectively. The user reported less “push” torque during stance phase when using the PD control. Tests with higher PD gains were also conducted. It was found that the large tracking error of stance phase can not be reduced even with doubled PD gains. To summarize, with all the discussion above, we can conclude that the MIQP+Imp controller has the best balanced performance between tracking and power requirements.

V. CONCLUSIONS

By leveraging a systematic methodology—including gait generation and real-time optimization based controllers—the first contribution of this paper was to extend this framework to experimentally realize stable prosthetic stair climbing. The

TABLE I: Experiment Results Comparison.

Control		e_{rms} [rad]	e_{max} [rad]	μ_{max} [Nm]	P [W]
PD	Ankle	0.0548	0.1218	37.200	6.0810
	Knee	0.1336	0.5282	72.741	43.022
PD+Imp	Ankle	0.0324	0.0896	30.3736	6.5867
	Knee	0.2054	0.7787	60.232	60.236
MIQPL+Imp	Ankle	0.0250	0.1301	15.747	5.4835
	Knee	0.0614	0.4185	50.072	51.656
MIQPH+Imp	Ankle	0.0255	0.1236	16.404	5.363
	Knee	0.0730	0.4114	66.117	54.389

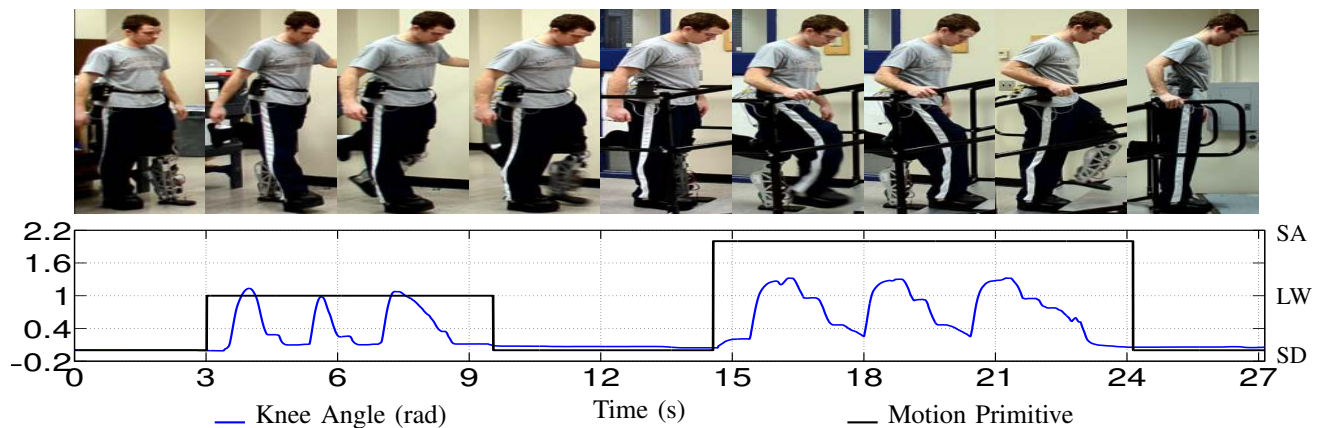


Fig. 5: Gait tiles (top) of switching between three motion primitives: standing, walking and stair ascent. The bottom figure illustrates the specific primitive at specific given time (right axis) together with the real-time knee angle (left axis).

performance of multiple controllers—utilizing the generated robotic walking inspired by the reference trajectories—are compared, with the real-time optimization based controller resulting in the best overall performance. The second contribution of this paper was a simple and effective motion recognition algorithm, which is utilized to experimentally achieve non-stop, smooth, automatic and natural motion transitions between a variety of behaviors with high accuracy. Future work will focus on multi-contact walking gaits for more natural human-like locomotion, higher staircases with a second generation prosthesis, and motion intent recognition algorithms utilizing only information on prosthetic device.

ACKNOWLEDGMENT

This research is supported under: NSF CAREER Award CNS-0953823 and Texas Emerging Technology Fund 11062-013. This research has approval from the Institutional Review Board with IRB2014-0382F for testing with humans.

REFERENCES

- [1] T. R. Dillingham, L. E. Pezzin, and E. J. MacKenzie, "Limb amputation and limb deficiency: epidemiology and recent trends in the united states." *Southern medical journal*, vol. 95, no. 8, pp. 875–883, 2002.
- [2] D. A. Winter, *Biomechanics and Motor Control of Human Movement*, 2nd ed. New York: Wiley-Interscience, May 1990.
- [3] S. Au, M. Berniker, and H. Herr, "Powered ankle-foot prosthesis to assist level-ground and stair-descent gaits," *Neural Networks*, vol. 21, no. 4, pp. 654 – 666, 2008.
- [4] J. A. Blaya and H. Herr, "Adaptive control of a variable-impedance ankle-foot orthosis to assist drop-foot gait," *Neural Systems and Rehabilitation Engineering, IEEE Transactions on*, vol. 12, no. 1, pp. 24–31, 2004.
- [5] F. Sup, A. Bohara, and M. Goldfarb, "Design and Control of a Powered Transfemoral Prosthesis." *The International journal of robotics research*, vol. 27, no. 2, pp. 263–273, Feb. 2008.
- [6] B. Lawson, H. Varol, A. Huff, E. Erdemir, and M. Goldfarb, "Control of stair ascent and descent with a powered transfemoral prosthesis," *Neural Systems and Rehabilitation Engineering, IEEE Transactions on*, vol. 21, no. 3, pp. 466–473, May 2013.
- [7] A. Young, A. Simon, and L. Hargrove, "A training method for locomotion mode prediction using powered lower limb prostheses," *Neural Systems and Rehabilitation Engineering, IEEE Transactions on*, vol. 22, no. 3, pp. 671–677, May 2014.
- [8] H. Zhao, J. Reher, J. Horn, V. Paredes, and A. D. Ames, "Realization of nonlinear real-time optimization based controllers on self-contained transfemoral prosthesis," in *6th International Conference on Cyber Physics System*, Seattle, WA, 2015.
- [9] H. Zhao, S. Kolathaya, and A. D. Ames, "Quadratic programming and impedance control for transfemoral prosthesis," in *International Conference on Robotics and Automation (ICRA)*, June 2014.
- [10] I. O. B. O. Ind., "Manual for the 3c100 otto bock c-leg," Duderstadt, Germany, 1998.
- [11] H. A. Varol, F. Sup, and M. Goldfarb, "Multiclass real-time intent recognition of a powered lower limb prosthesis," *Biomedical Engineering, IEEE Transactions on*, vol. 57, no. 3, pp. 542–551, 2010.
- [12] H. Huang, F. Zhang, L. Hargrove, Z. Dou, D. Rogers, and K. Englehart, "Continuous locomotion-mode identification for prosthetic legs based on neuromuscular-mechanical fusion," *Biomedical Engineering, IEEE Transactions on*, vol. 58, no. 10, pp. 2867–2875, 2011.
- [13] S. Šljajpah, R. Kamnik, and M. Munih, "Kinematics based sensory fusion for wearable motion assessment in human walking," *Computer methods and programs in biomedicine*, 2013.
- [14] H. Zhao, M. Powell, and A. D. Ames, "Human-inspired motion primitives and transitions for bipedal robotic locomotion in diverse terrain," *Optimal Control Applications and Methods*, vol. 35, no. 6, pp. 730–755, 2014.
- [15] A. D. Ames, "Human-inspired control of bipedal walking robots," *Automatic Control, IEEE Transactions on*, vol. 59, no. 5, pp. 1115–1130, 2014.
- [16] W.-L. Ma, H. Zhao, S. Kolathaya, and A. D. Ames, "Human-inspired walking via unified pd and impedance control," in *submitted to the IEEE International Conference on Robotics and Automation*, 2014.
- [17] H. Zhao, W.-L. Ma, M. Zeagler, and A. D. Ames, "Human-inspired multi-contact locomotion with amber2," in *Cyber-Physical Systems (ICCPs), International Conference on*, April 2014, pp. 199–210.
- [18] T. S. Parker, L. O. Chua, and T. S. Parker, *Practical numerical algorithms for chaotic systems*. Springer New York, 1989.
- [19] A. D. Ames, K. Galloway, K. Sreenath, and J. W. Grizzle, "Rapidly exponentially stabilizing control lyapunov functions and hybrid zero dynamics," *Automatic Control, IEEE Transactions on*, vol. 59, no. 4, pp. 876–891, 2014.
- [20] H. Zhao and A. D. Ames, "Quadratic program based control of fully-actuated transfemoral prosthesis for flat-ground and up-slope locomotion," in *American Control Conference*, 2014, pp. 4101–4107.
- [21] G. Zhang, "Neural networks for classification: a survey," *Systems, Man, and Cybernetics, Part C: Applications and Reviews, IEEE Transactions on*, vol. 30, no. 4, pp. 451–462, Nov 2000.
- [22] Realization of Stair Ascent and Motion Transitions with AMPRO. <https://youtu.be/oNZxkiiCnUg>.